

QCD with light Wilson quarks on fine lattices (I): first experiences and physics results

L. Del Debbio¹, L. Giusti^{2,*}, M. Lüscher², R. Petronzio³, N. Tantalo^{3,4}

¹*SUPA, School of Physics, University of Edinburgh, Edinburgh EH9 3JZ, UK*

²*CERN, Physics Department, TH Division, CH-1211 Geneva 23, Switzerland*

³*Università di Roma “Tor Vergata” and INFN sezione “Tor Vergata”,
Via della Ricerca Scientifica 1, I-00133 Rome, Italy*

⁴*Centro Enrico Fermi, Via Panisperna 89 A, I-00184 Rome, Italy*

Abstract

Recent conceptual, algorithmic and technical advances allow numerical simulations of lattice QCD with Wilson quarks to be performed at significantly smaller quark masses than was possible before. Here we report on simulations of two-flavour QCD at sea-quark masses from slightly above to approximately 1/4 of the strange-quark mass, on lattices with up to 64×32^3 points and spacings from 0.05 to 0.08 fm. Physical sea-quark effects are clearly seen on these lattices, while the lattice effects appear to be quite small, even without $O(a)$ improvement. A striking result is that the dependence of the pion mass on the sea-quark mass is accurately described by leading-order chiral perturbation theory up to meson masses of about 500 MeV.

1. Introduction

Many different formulations of lattice QCD are currently in use. The aim to reduce the lattice effects and to preserve chiral symmetry as much as possible has been the principal motivation for the introduction of increasingly complicated lattice actions. Highly improved actions are not obviously the best choice in practice, however, since they tend to slow down the numerical simulations by a large factor. Moreover, the

* On leave from Centre de Physique Théorique, CNRS Luminy, F-13288 Marseille, France

conceptual transparency of the lattice theory (otherwise one of its greatest assets) may be compromised in extreme cases.

The philosophy advocated here is to keep the theory simple at the fundamental level (thus sticking to Wilson’s formulation [1] and its close relatives) and to develop adapted computational strategies that allow simulations of large lattices with small spacings to be performed efficiently. Extrapolations to the continuum limit will then still be required, but the hope is that, in many cases of interest, the lattice effects will already be small at the accessible lattice spacings.

For many years, the Wilson theory had the reputation of being difficult to simulate at light-quark masses significantly smaller than half the strange-quark mass. The situation has now changed completely, following the development of the DD-HMC simulation algorithm [2–4] and of a fine-tuned version of the Hasenbusch-accelerated HMC algorithm [5–8], both being much faster than the algorithms used thus far (for related earlier studies of unquenched lattice QCD, see refs. [9–14], for example). The success of these algorithms is partly also due to the fact, discovered later [15], that the Wilson–Dirac operator has a safe spectral gap in the large-volume regime of QCD, even though chiral symmetry is not exact in the Wilson theory.

In this paper we report on extensive simulations of two-flavour QCD in a range of lattice spacings, lattice sizes and quark masses not explored before. Apart from sect. 2, where the simulations are briefly described, the emphasis is put on the main physics results. Further details of the simulations, data tables, etc., will be published in a forthcoming more technical paper.

2. Simulation table

As already indicated, the lattice theory is set up following Wilson [1], with a doublet of sea quarks of equal mass. In this theory, the sea quarks represent the up and down quarks, while the strange quark will be added later, at the level of a valence quark, i.e. without the associated quark determinant.

Three series of lattices were simulated, labelled A , B and D (see table 1) [†]. In the D series, the Sheikholeslami–Wohlert term [16] was included in the quark action with coefficient c_{sw} set to the value determined by the ALPHA collaboration [18], thus ensuring non-perturbative on-shell $\mathcal{O}(a)$ improvement. The size of the representative

[†] Our notation and normalization conventions coincide with those of ref. [17]. As usual we quote the values of $\beta = 6/g_0^2$ and $\kappa = 8 + 2m_0$ instead of the bare coupling g_0 and sea-quark mass m_0 .

Table 1. Simulations included in the physics analysis

Run	Lattice	β	c_{sw}	κ	N_{cfg}
A_1	32×24^3	5.6	0	0.15750	64
A_2				0.15800	109
A_3				0.15825	100
B_1	64×32^3	5.8	0	0.15410	100
B_2				0.15440	101
B_3				0.15455	104
B_4				0.15462	102
D_1	48×24^3	5.3	1.90952	0.13550	104
D_2				0.13590	171
D_3				0.13610	168
D_4				0.13620	168
D_5				0.13625	169

ensemble of gauge-field configurations generated in each case is given in the last column of table 1.

In physical units, the lattice spacing on the A , B and D lattices is estimated to be 0.0717(15), 0.0521(7) and 0.0784(10) fm respectively (see sect. 4). The three series of simulations cover a similar range of sea-quark masses, from values slightly above the strange-quark mass m_s down to values close to $m_s/4$.

All simulations were performed using the DD-HMC algorithm [4], which combines domain decomposition ideas with the Hybrid-Monte-Carlo algorithm [19] (hence the name DD-HMC). As explained in refs. [4,21], the speed of the algorithm also very much depends on the use of the Sexton–Weingarten multiple-time integration scheme [20]. In practice, a relevant performance figure is the number N_{op} of floating-point operations required for the generation of an ensemble of 100 statistically independent field configurations on a $2L \times L^3$ lattice at a specified lattice spacing and sea-quark mass. A formula that fits our experience with the DD-HMC algorithm well is

$$N_{\text{op}} = k \left(\frac{20 \text{ MeV}}{\overline{m}} \right) \left(\frac{L}{3 \text{ fm}} \right)^5 \left(\frac{0.1 \text{ fm}}{a} \right)^6 \text{ Tflops} \times \text{year}, \quad (2.1)$$

where \overline{m} denotes the running sea-quark mass in the $\overline{\text{MS}}$ scheme at renormalization

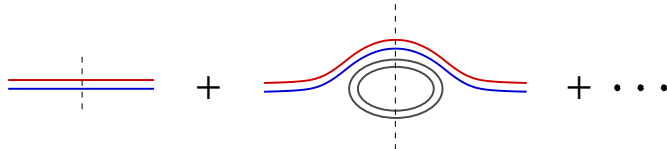


Fig. 1. Quark-line diagrams contributing to the two-point correlation function (3.1). In the second diagram, two pairs of sea-quarks are created from the vacuum and bind into a pair of pseudo-scalar mesons.

scale $\mu = 2$ GeV and $k \simeq 0.05$ if the $O(a)$ -improved theory is simulated ($k \simeq 0.03$ without improvement).

In 2001, at the annual conference on lattice field theory in Berlin, a similar formula was presented by Ukawa [22], summarizing the experience made by the CP-PACS and JLQCD collaborations with the algorithms available at the time. With respect to that formula, the scaling exponent of the quark mass in eq. (2.1) is reduced from 3 to 1, the exponent of the lattice spacing from 7 to 6, and the constant k is roughly 100 times smaller.

Apart from the operations count, the suitability of the simulation algorithm for parallel processing is a key issue, if large lattices are to be simulated. Domain decomposition methods tend to perform well from this point of view, and one of the design goals of the DD-HMC algorithm was in fact to keep the communication overhead small [3,4]. Special-purpose computers are then not required and most simulations (including the B series) were actually performed on commodity PC clusters with up to 64 double-processor nodes[†].

3. Physical sea-quark effects

Once the sea quarks are included in the simulations, an obvious question is whether their presence has a visible effect on the computed quantities. Correlation functions of local fields depend on the sea-quark content of the theory in various ways. The flavoured pseudo-scalar densities, for example, can only couple to multi-meson states through the creation of virtual quark pairs (see fig. 1). Higher-states contributions to the correlation functions of these fields are therefore expected to increase when the sea-quark mass is lowered (thus moving away from quenched QCD).

[†] The program that was used for the simulations of the $O(a)$ -improved theory (the D series) can be downloaded from <http://cern.ch/luscher/DD-HMC>.

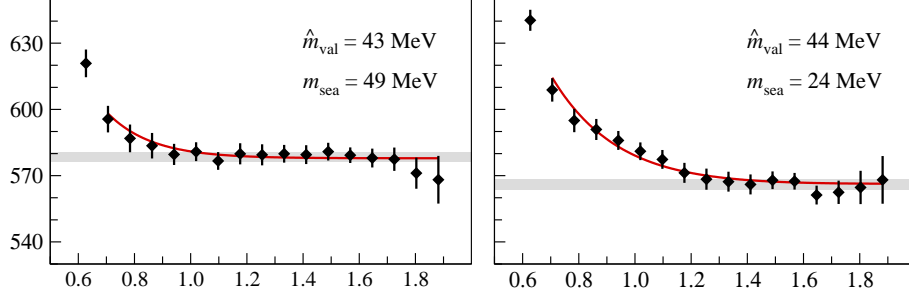


Fig. 2. Simulation results (data points) for the effective pseudo-scalar mass $M_{\text{eff}}(t)$ in MeV as a function of the time t in fm (runs D_2 and D_4). The average valence-quark masses \hat{m}_{val} and the meson masses M (grey bands) are nearly the same in the two cases, while the sea-quark mass m_{sea} changes by a factor of 2 (quoted quark masses are bare current-quark masses).

Indications for the presence of multi-meson intermediate states in some two-point correlation functions were already found some time ago by the UKQCD collaboration [23]. We now have data at smaller quark masses, where the effect is more pronounced and where a significant dependence on the sea-quark mass is seen in both the pseudo-scalar and vector channels.

For illustration we introduce two valence quarks, labelled r and s , and consider the two-point correlation function

$$C(t) = - \int_{x_0=t} d^3x \langle (\bar{r} \gamma_5 s)(x) (\bar{s} \gamma_5 r)(0) \rangle \quad (3.1)$$

of the corresponding flavoured pseudo-scalar density at zero spatial momentum (for simplicity we use a continuum notation in this section). In finite volume, $C(t)$ may be expanded in a spectral series

$$C(t) \underset{t \rightarrow \infty}{=} c_0 e^{-Mt} + c_1 e^{-M't} + \dots, \quad (3.2)$$

where M denotes the mass of the associated pseudo-scalar meson and M' the energy of a three-meson state with all particles at rest.

Plots of the effective mass

$$M_{\text{eff}}(t) = - \frac{d}{dt} \ln C(t) = M + c e^{-(M'-M)t} + \dots \quad (3.3)$$

now show that the higher-states contributions are not small in general. Moreover, as is evident from fig. 2, they tend to grow when the sea quarks become lighter. In

the cases shown in the figure, the energy M' of the lowest three-meson intermediate state is expected to be approximately equal to $M + 2M_\pi$, where M_π denotes the mass of the pseudo-scalar mesons made of the sea quarks. The two-state formula (3.3) actually fits the data quite well if this expression is assumed and if M_π is determined from the sea-quark pseudo-scalar correlation function (solid lines in fig. 2).

While the observed enhancement of higher-states contributions is in line with qualitative theoretical expectations, their presence also tends to complicate the analysis of the simulation data. In particular, at small sea-quark masses, the computation of hadron masses may require accurate data at larger time separations than was the case in quenched QCD. Multi-mass fits and variational methods can be helpful at this point, although the associated systematic uncertainties must then be balanced against the possibly lower statistical errors.

4. Setting the scale

The choice of a physical reference scale is an important step in the analysis of the simulation data. Results obtained on different lattices can then be expressed in units of this scale and thus be compared with one another.

Following ref. [17], we adopt a mass-independent scheme where the lattice spacing in physical units is the same on all lattices at a given bare coupling. Different choices of the reference scale are possible, none of which appears to be free of some practical or conceptual shortcoming. Here we add a valence strange quark to the theory and determine the scale through the pion mass and the masses of the pseudo-scalar and vector mesons that are made of a strange antiquark and a sea quark (we refer to these as the K and the K^*). More precisely, we adjust the quark masses so that the ratios M_K/M_{K^*} and M_π/M_K assume some prescribed values and then take M_K as the reference scale.

Since we wish to set the scale in a physically sensible way, we require the ratio M_K/M_{K^*} to be equal to its physical value of 0.554. This condition fixes the strange-quark mass m_s at any given coupling and sea-quark mass m (see fig. 3). Ideally we would like the latter to be such that M_π/M_K assumes its physical value too, but this would require a long extrapolation in the sea-quark mass and, moreover, would be a point where the K^* is unstable (i.e. the extrapolation would have to go through a kinematical threshold).

We now note, however, that once m_s is fixed, the reference scale in lattice units, aM_K , appears to be weakly dependent on m , particularly so at small m (see fig. 3).

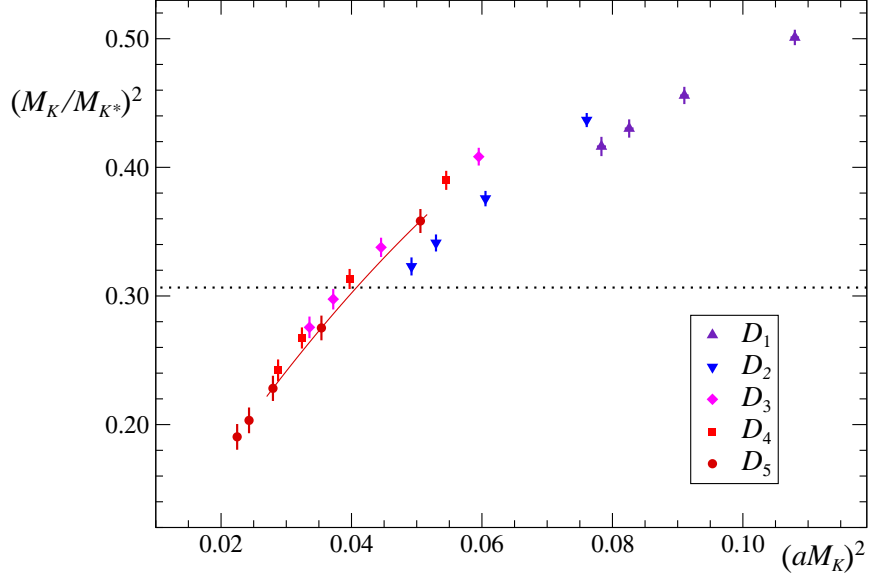


Fig. 3. On each lattice, the masses of the K and the K^* were computed at 4 or 5 values of the bare strange-quark mass. The results obtained on the D lattices are plotted here for illustration (data points). At the lighter sea-quark masses, the point where $M_K/M_{K^*} = 0.554$ (dotted line) is found by a quadratic interpolation in the strange-quark mass of the nearest data points. The solid line shows the interpolation in the case of the lattice D_5 .

The reason for this behaviour (which is seen on all series of lattices) could be that both M_K and M_{K^*} are functions of $m + m_s$ rather than of m and m_s separately, up to corrections proportional to the squares of the masses. In any case, the observation suggests the reference scale to be defined at the point where, say, $M_\pi/M_K = 0.85$, which is within the available data range. This convention, although somewhat unphysical, is entirely satisfactory for the purpose of comparing results from different lattices.

The results for the reference scale obtained in this way are summarized in table 2. In order to avoid any confusions, we mark all quantities evaluated at the reference point with a subscript “ref”. The sea-quark and strange-quark hopping parameters at the reference point, for example, are denoted by κ_{ref} and $\kappa_{s,\text{ref}}$. Setting $M_{K,\text{ref}} = 495$ MeV, this leads to the lattice spacings quoted in the last column of the table, while for the pion masses at the smallest sea-quark masses on the A , B and D series of lattices we obtain 403, 381 and 377 MeV respectively.

The lattice spacings calculated here are significantly smaller than those previously

Table 2. Determination of the lattice spacing*

Lattice series	κ_{ref}	$\kappa_{s,\text{ref}}$	$aM_{K,\text{ref}}$	a [fm]
<i>A</i>	0.15822(3)	0.15769(4)	0.180(4)	0.0717(15)
<i>B</i>	0.154561(12)	0.154257(10)	0.1310(17)	0.0521(7)
<i>D</i>	0.136207(7)	0.135912(13)	0.197(3)	0.0784(10)

* At the quark masses where $M_K/M_{K^*} = 0.554$ and $M_\pi/M_K = 0.85$

published by us in a conference report [21], where the Sommer radius [24] was used as reference scale. Larger lattice spacings are also obtained if the scale is set by the K and K^* masses, similarly to what was done here, but at larger sea-quark masses (see fig. 3). As a result of the new determination of the lattice spacings, our estimates of the pion masses in MeV are pushed to higher values than those quoted in ref. [21]. Moreover, we decided to discard the simulation at the lightest quark mass reported there, because the lattice turned out to be too small for that mass.

All this illustrates the fact that at present the assignment of physical units remains somewhat ambiguous. For a definitive solution of the problem, simulations at smaller quark masses will probably be required, and the scale setting may eventually have to be based on the properties of the stable hadrons (the pion and the nucleon in the two-flavour theory).

5. Quark-mass dependence of M_π and F_π

The bare quark masses that appear in the lattice action of the Wilson theory require a power-divergent additive renormalization. This complication can be bypassed by extracting the quark masses from the PCAC relation (see ref. [17], for example; in the improved theory, we used the non-perturbatively improved axial current [25]). Moreover, ratios of these masses do not need to be renormalized since the multiplicative renormalization factor cancels.

In fig. 4 the ratio $(M_\pi/M_{K,\text{ref}})^2$ is plotted as a function of the corresponding ratio of quark masses. If there were no systematic effects, all data points shown in this figure would have to lie on a single curve, within statistical errors, representing the mass dependence of $(M_\pi/M_{K,\text{ref}})^2$ in the continuum limit. Note that the statistical

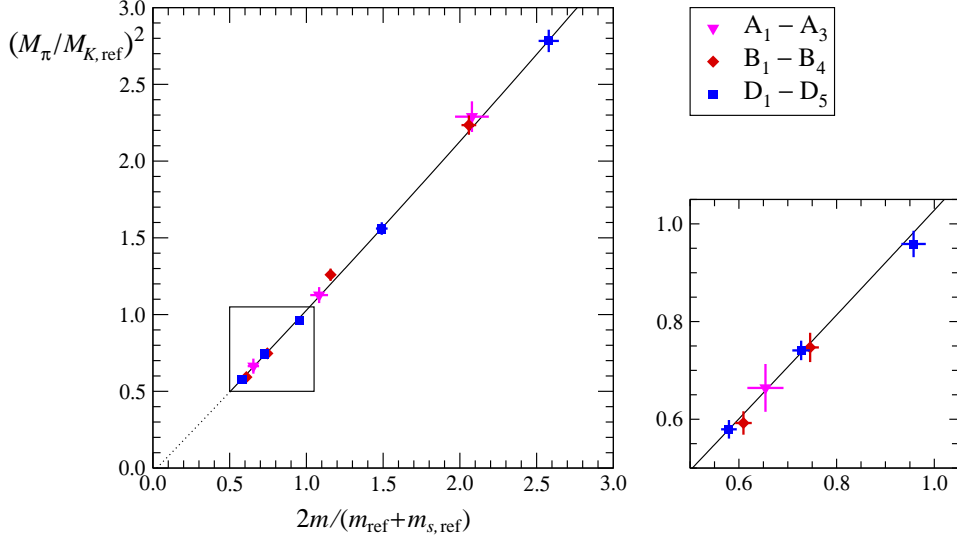


Fig. 4. Dependence of the square of the pion mass M_π on the sea-quark mass m . The solid curve is a quadratic least-squares fit (with constant term) of all data points, and the plot on the right is a blowup of the region enclosed by the little box.

errors of the points are uncorrelated, except for the correlations that are introduced through the normalization factors. The quality of the empirical fit (solid line) then suggests that no statistically significant systematic effects are seen in this plot.

Another rather striking outcome is that M_π^2 is a nearly linear function of the sea-quark mass m in the range covered by the data. There is a visible curvature towards the larger masses in fig. 4, but the coefficient of the quadratic term in the empirical fit, $y = -0.03(3) + 1.03(5)x + 0.02(2)x^2$, is small. In the range $M_\pi/M_{K,\text{ref}} \leq 1.1$, the data are also well represented by a straight line through the origin.

The corresponding plot of the pion decay constant F_π , given in units of the decay constant $F_{K,\text{ref}}$ of the K meson at the reference point, is more difficult to interpret (see fig. 5). Apart from the fact that the statistical errors tend to be larger here, the results of the D series of simulations appear to be significantly different from those of the A and B series. There is no obvious curvature in either set of data points, and correlated straight-line fits (solid lines) are found to be statistically consistent. Although the two lines are visibly different, the fitted values of their slopes, $0.235(11)$ and $0.192(11)$, deviate from each other by less than 3 times the combined statistical error. The statistical significance of the effect is thus not overwhelming.

When discussing systematic errors, an important point to note is that the axial-current renormalization constant Z_A cancels in the ratio of decay constants plotted

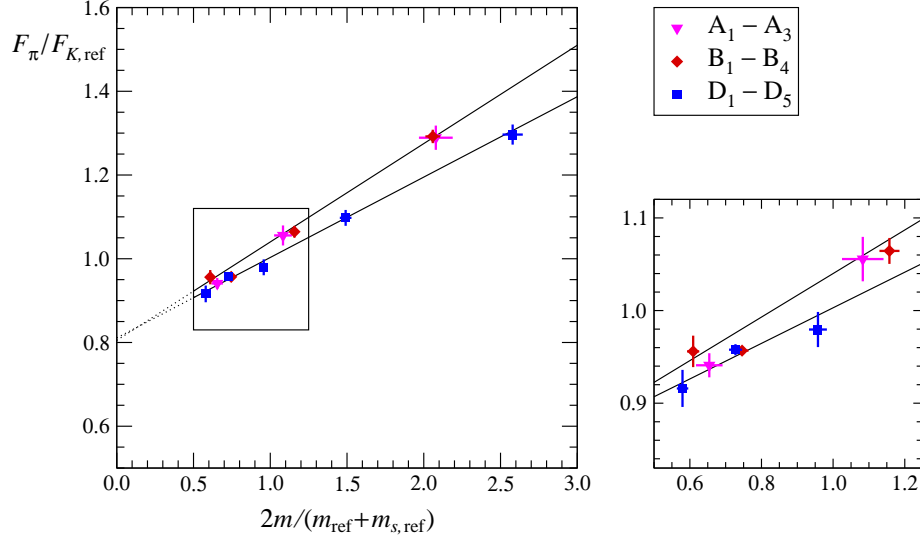


Fig. 5. Dependence of the pion decay constant F_π on the sea-quark mass m . The solid curves are linear least-squares fits of the data points from the A and B lattices (upper line) and of the points from the D lattices (lower line).

in fig. 5. Moreover, the ratio is largely insensitive to the values of the improvement coefficients c_A and b_A [17,25] on which the axial current in the $O(a)$ improved theory depends. Lattice effects may still be significant, however, and we can also not exclude the presence of important finite-volume effects. A more specific problem is that any variations in the normalization factors $F_{K,\text{ref}}$ and $m_{\text{ref}} + m_{s,\text{ref}}$ propagate to the slopes of the lines in fig. 5. The alignment of the data points may therefore appear to be better or worse, depending on the statistical fluctuations at the reference point and on its detailed specification.

The fact that the lines in fig. 5 have nearly the same intercept in the chiral limit is probably an accident. Both lines also practically pass through $F_\pi/F_{K,\text{ref}} = 0.82$ (the experimental value of F_π/F_K) at $M_\pi/M_{K,\text{ref}} = 0.28$. However, as will be shown in the next section, such extrapolations to smaller quark masses could be misleading.

6. Comparison with chiral perturbation theory

In two-flavour QCD with unbroken isospin symmetry, the chiral expansion of the

pion mass reads [26]

$$M_\pi^2 = M^2 + \frac{M^4}{32\pi^2 F^2} \ln(M^2/\Lambda_3^2) + \dots, \quad M^2 \equiv 2Bm, \quad (6.1)$$

where F , B and Λ_3 are a priori unknown constants. A phenomenological analysis, taking low-energy experimental data as input, suggests [26,27]

$$F = 86.2 \pm 0.5 \text{ MeV}, \quad \bar{l}_3 \equiv \ln(\Lambda_3^2/M^2)|_{M=139.6 \text{ MeV}} = 2.9 \pm 2.4, \quad (6.2)$$

while B depends on the renormalization scheme for the quark mass and thus cannot be determined from such data alone. The chiral expansion of the pion decay constant has the form [26]

$$F_\pi = F - \frac{M^2}{16\pi^2 F} \ln(M^2/\Lambda_4^2) + \dots \quad (6.3)$$

and the phenomenological discussion leads to the estimate [28]

$$\bar{l}_4 \equiv \ln(\Lambda_4^2/M^2)|_{M=139.6 \text{ MeV}} = 4.4 \pm 0.2 \quad (6.4)$$

for the low-energy constant Λ_4 .

In principle the low-energy constants can be determined from lattice data without recourse to phenomenological estimates. However, as will become clear shortly, the available simulation data are insufficient for a solid analysis of this kind. While the situation in the case of the pion mass is somewhat more favourable, our principal goal in the following will be to find out whether the data are compatible with the expansions (6.1) and (6.3) for a reasonable choice of the parameters.

We first need to rewrite the equations in a form where all dimensioned quantities are expressed in units of the scales at the reference point. To this end, it is helpful to introduce the abbreviations

$$x = \frac{2m}{m_{\text{ref}} + m_{s,\text{ref}}}, \quad C = \frac{M_{K,\text{ref}}^2}{32\pi^2 F_{K,\text{ref}}^2}, \quad (6.5)$$

and to define the scaled parameters

$$\hat{F} = \frac{F}{F_{K,\text{ref}}}, \quad \hat{B} = \frac{m_{\text{ref}} + m_{s,\text{ref}}}{M_{K,\text{ref}}^2} B, \quad \hat{l}_n = \ln(\Lambda_n^2/M_{K,\text{ref}}^2). \quad (6.6)$$

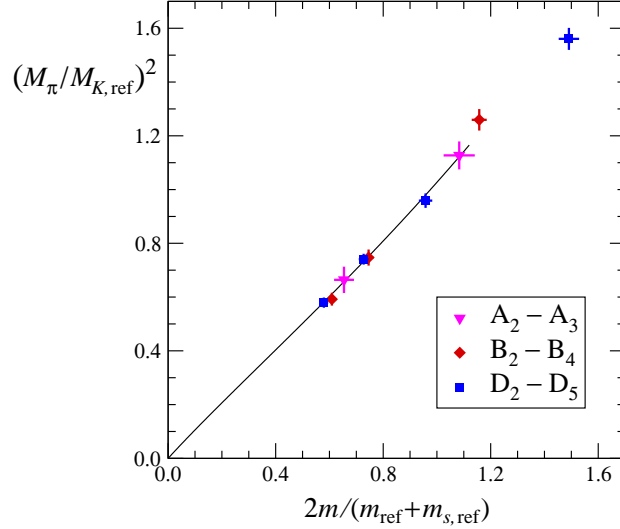


Fig. 6. Fit of the quark-mass dependence of the square of the pion mass M_π in the range $M_\pi/M_{K,\text{ref}} \leq 1.1$, using the one-loop formula (6.7) with $C = 0.072$ and $\hat{F} = 0.70$ (solid line). The fit is a correlated least-squares fit of all data points in the specified range, with unconstrained parameters \hat{B} and \hat{l}_3 .

The chiral expansions

$$\frac{M_\pi^2}{M_{K,\text{ref}}^2} = \hat{B}x + C \frac{\hat{B}^2 x^2}{\hat{F}^2} \{ \ln(\hat{B}x) - \hat{l}_3 \} + \dots, \quad (6.7)$$

$$\frac{F_\pi}{F_{K,\text{ref}}} = \hat{F} - 2C \frac{\hat{B}x}{\hat{F}} \{ \ln(\hat{B}x) - \hat{l}_4 \} + \dots, \quad (6.8)$$

may now be directly compared with the simulation data (note that $\hat{l}_n = \bar{l}_n - 2.53$ if $M_{K,\text{ref}} = 495$ MeV is assumed).

The computation of the decay constant $F_{K,\text{ref}}$, and thus of the constant C , involves the renormalization constant Z_A of the axial current. Recent estimates of the latter in the two-flavour Wilson theory at the couplings of the A and B lattices are 0.77(2) and 0.78(2) [29], while in the case of the D series of lattices we may use the value 0.75(1) determined by the ALPHA collaboration [30]. For the constant C we then find 0.068(4), 0.071(4) and 0.076(3) respectively. These figures are barely consistent with one another, suggesting the presence of lattice or finite-volume effects, but it should also be noted that the determination of Z_A is not free of systematic

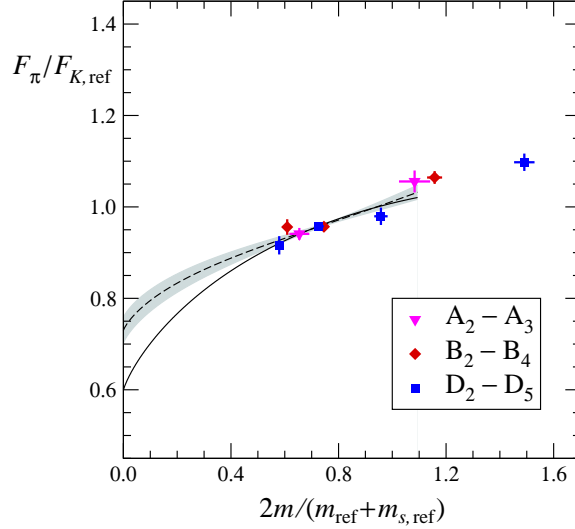


Fig. 7. Fit of the quark-mass dependence of the pion decay constant F_π in the range $M_\pi/M_{K,\text{ref}} \leq 1.1$, using the one-loop formula (6.8) with $C = 0.072$ and $\hat{B} = 1.106$ (solid line). The dashed line with its 1-sigma error margin (grey band) represents an alternative fit that includes a hypothetical two-loop term.

ambiguities [29,30] [†].

A very accurate determination of C is fortunately not needed for the chiral fits, because C only appears at next-to-leading order in the chiral expansions. We thus set $C = 0.072$ and simplify the fit procedure by substituting $\hat{F} = 0.70$ in eq. (6.7), which will turn out to be an approximately correct value. In the range $M_\pi/M_{K,\text{ref}} \leq 1.1$, the one-loop formula (6.7) then fits the data for the pion mass very well, the fit parameters being $\hat{B} = 1.11(6)(3)$ and $\hat{l}_3 = 0.5(5)(1)$ (see fig. 6; the second errors are estimates of the systematic uncertainty arising from the inaccurately known values of C and \hat{F}). We did not attempt to estimate the effects of any higher-order terms in eq. (6.7) so that the quoted values of the fit parameters should be taken as effective values, describing the data in the specified range of pion masses.

In the case of the pion decay constant, the comparison of the simulation data with the chiral formula (6.8) is complicated by the scattering of the data points in fig. 5, which may partly be the result of systematic effects. However, since the points line

[†] The same comments apply in the case of $F_{K,\text{ref}}$ where we obtain 107(3), 105(3) and 101(2) MeV on the A , B and D lattices (assuming $M_{K,\text{ref}} = 495$ MeV as before). The fact that these results are all lower than the decay constant $F_K = 113(1)$ MeV of the physical kaon may not be significant, because the two-flavour theory neglects the effects of the strange sea quark.

up at the smaller quark masses, we may attempt to fit these, setting C and \hat{B} to the previously determined values and adjusting \hat{F} and \hat{l}_4 (see fig. 7). The statistical quality of this fit (solid line) turns out to be quite good, but the curvature of the fit function is not seen in the data and the fit therefore appears to be somewhat artificial.

A more plausible fit (dashed line) can be obtained by including a hypothetical two-loop term proportional to $\hat{B}^2 x^2 / \hat{F}^3$ in the chiral expansion (6.8), with a coefficient $C' = 0.046$ that is not unreasonably large. The fit parameters \hat{F} and \hat{l}_4 change from $0.60(4)$ and $1.6(1)$ to $0.73(3)$ and $0.73(8)$, respectively, when the two-loop term is added.

The discussion in this section shows that simulation data at significantly smaller quark masses, with small systematic and statistical errors, will be required for a reliable determination of the parameters in the chiral lagrangian. It seems safe to conclude, however, that our results in the range $M_\pi/M_{K,\text{ref}} \leq 1.1$ are not incompatible with chiral perturbation theory. In particular, the fact that M_π^2 is a nearly linear function of the quark mass m is not in conflict with the presence of the chiral logarithm in eq. (6.7).

7. Concluding remarks

In the coming years, simulations of lattice QCD with Wilson quarks will no doubt rapidly progress towards smaller quark masses and lattice spacings than are reported here. In order to guarantee the stability of the simulations [15], but also to keep the finite-volume effects under control, the constraints

$$M_\pi L \geq 3, \quad L \geq 2 \text{ fm}, \quad (7.1)$$

should be respected in these computations. On a given lattice, the bounds (7.1) set a lower limit on the lattice spacings and pion masses that can be reached (see fig. 8). Simulations of the two-flavour theory may not be practical at all these points, but the cost formula (2.1) is encouraging and suggests that simulations at $a \leq 0.08$ fm and $M_\pi \leq 300$ MeV, for example, can be performed already with the computer resources available at present. However, to be able to sort out the systematic errors, many lattices will have to be simulated which may require a coordinated effort.

On the A , B and D series of lattices, the smallest values of $M_\pi L$ are 3.5, 3.2 and 3.6 respectively, while the spatial sizes L of the lattices are estimated to be 1.72, 1.67

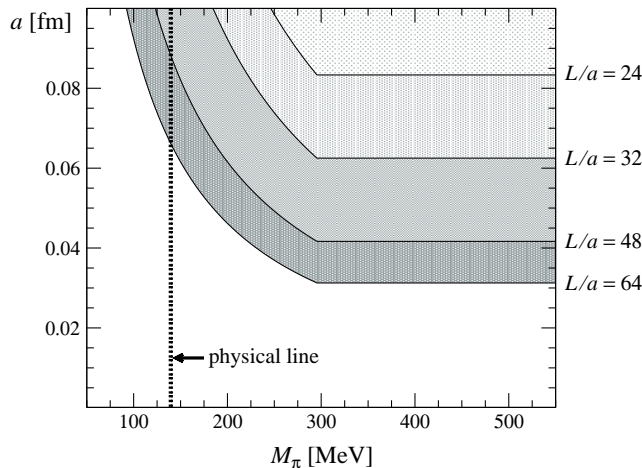


Fig. 8. Range of lattice spacings a and pion masses M_π defined by the bounds (7.1) on a $2L \times L^3$ lattice as a function of the lattice size L/a (shaded area above the line labelled by the corresponding value of L/a).

and 1.88 fm, i.e. somewhat below the required minimum. Finite-volume effects may not be totally negligible on these lattices and will need to be investigated, extending the studies by Orth et al. [14] to smaller quark masses and lattice spacings. So far we did not include the nucleons in the physics analysis, because these are probably even more sensitive to finite-volume effects than the mesons.

It may be somewhat surprising that no significant lattice effects were seen in fig. 4, even though $O(a)$ counterterms were only included in the D series of simulations. The weak dependence on the lattice spacing could be related to the fact, first noted by Sharpe and Singleton [31], that the $O(a)$ lattice effects amount to an additive quark-mass renormalization at leading order of chiral perturbation theory. Since the quark masses that appear in the PCAC relation already include all additive renormalizations, it follows that the data points plotted in fig. 4 are insensitive to these leading-order lattice effects.

The mass dependence of the pseudo-scalar decay constant, on the other hand, is a second-order effect in chiral perturbation theory. At this order, only some of the $O(a)$ lattice corrections can be compensated by a renormalization of the parameters in the chiral lagrangian, and an accidental $O(a)$ improvement is therefore not expected in this case.

We wish to thank Rainer Sommer for technical discussions and Gilberto Colangelo, Stephan Dür, Jürg Gasser and Heiri Leutwyler for some very helpful notes, summarizing some relevant results of chiral perturbation theory. The numerical simulations

were performed on PC clusters at CERN, the Centro Enrico Fermi, the Institut für Theoretische Physik der Universität Bern (with a contribution from the Schweizerischer Nationalfonds) and on a CRAY XT3 at the Swiss National Supercomputing Centre (CSCS). We are grateful to all these institutions for the continuous support given to this project.

References

- [1] K. G. Wilson, Phys. Rev. D10 (1974) 2445
- [2] M. Lüscher, JHEP 0305 (2003) 052
- [3] M. Lüscher, Comput. Phys. Commun. 156 (2004) 209
- [4] M. Lüscher, Comput. Phys. Commun. 165 (2005) 199
- [5] M. Hasenbusch, Phys. Lett. B519 (2001) 177
- [6] M. Hasenbusch, K. Jansen, Nucl. Phys. B659 (2003) 299
- [7] M. Della Morte et al. (ALPHA collab.), Comput. Phys. Commun. 156 (2003) 62
- [8] C. Urbach, K. Jansen, A. Shindler, U. Wenger, Comput. Phys. Commun. 174 (2006) 87
- [9] N. Eicker et al. (SESAM collab.), Phys. Rev. D59 (1999) 014509
- [10] C. R. Allton et al. (UKQCD collab.), Phys. Rev. D60 (1999) 034507; *ibid.* D65 (2002) 054502
- [11] A. Ali Khan et al. (CP-PACS collab.), Phys. Rev. Lett. 85 (2000) 4674 [E: *ibid.* 90 (2003) 029902]; Phys. Rev. D65 (2002) 054505 [E: *ibid.* D67 (2003) 059901]
- [12] S. Aoki et al. (JLQCD collab.) Phys. Rev. D68 (2003) 054502
- [13] Y. Namekawa et al. (CP-PACS collab.), Phys. Rev. D70 (2004) 074503
- [14] B. Orth, T. Lippert, K. Schilling, Phys. Rev. D72 (2005) 014503
- [15] L. Del Debbio, M. Lüscher, L. Giusti, R. Petronzio, N. Tantalo, JHEP 0602 (2006) 011
- [16] B. Sheikholeslami, R. Wohlert, Nucl. Phys. B259 (1985) 572
- [17] M. Lüscher, S. Sint, R. Sommer, P. Weisz, Nucl. Phys. B478 (1996) 365
- [18] K. Jansen, R. Sommer (ALPHA collab.), Nucl. Phys. B530 (1998) 185 [E: *ibid.* B643 (2002) 517]
- [19] S. Duane, A. D. Kennedy, B. J. Pendleton, D. Roweth, Phys. Lett. B195 (1987) 216
- [20] J. C. Sexton, D. H. Weingarten, Nucl. Phys. B380 (1992) 665

- [21] M. Lüscher, Lattice QCD with light Wilson quarks, in: Proceedings of the 23rd International Symposium on Lattice Field Theory, Dublin, 2005, eds. A. Irving, C. McNeile, C. Michael, PoS (LAT2005) 002
- [22] A. Ukawa, Nucl. Phys. B (Proc. Suppl.) 106–107 (2002) 195
- [23] C. R. Allton et al. (UKQCD collab.), Phys. Rev. D70 (2004) 014501
- [24] R. Sommer, Nucl. Phys. B411 (1994) 839
- [25] M. Della Morte, R. Hoffmann, R. Sommer, JHEP 0503 (2005) 029
- [26] J. Gasser, H. Leutwyler, Ann. Phys. 158 (1984) 142
- [27] G. Colangelo, S. Dürr, Eur. Phys. J. C 33 (2004) 543
- [28] G. Colangelo, J. Gasser, H. Leutwyler, Nucl. Phys. B603 (2001) 125
- [29] D. Bećirević et al. (SPQ_{CD}R collab.), Nucl. Phys. B734 (2006) 138
- [30] M. Della Morte et al. (ALPHA collab.), JHEP 0507 (2005) 007
- [31] S. R. Sharpe, R. L. Singleton, Phys. Rev. D58 (1998) 074501